## SUPPLEMENTAL INFORMATION

# Reviving B-factors: Activating ALK mutations increase protein dynamics of the unphosphorylated kinase

Ted W. Johnson,* Ben Bolanos, Alexei Brooun, Rebecca A. Gallego, Dan Gehlhaar, Mehran Jalaie, Michele McTigue, Sergei Timofeevski

Pfizer Worldwide Research and Development, La Jolla Oncology, 10770 Science Center Drive, San Diego, California 92121, United States

## METHODS

**Enzyme Kinetic Assays**. Recombinant human wildtype and mutant ALK kinase domain proteins (amino acids 1093−1411) were produced in house using baculoviral expression and optimally pre-activated by autophosphorylation similar as previously described.[1] The activated highly pure proteins (as verified by active site titrations with potent inhibitors) contained 3 to 4 phosphates per molecule by intact protein mass spectrometry analysis. Kinetic parameters were determined by a coupled spectrophotometric ATP-regenerating assay as previously reported[1-2] using the activation loop peptide analog, ARDIYRASFFRKGGCAMLPVK ("YFF") as a phosphoacceptor substrate, which was reported to be phosphorylated more rapidly than the wild-type "YYY" peptide.[3] The reactions contained 2.5−10 nM of activated or 50−300 nM non-activated wildtype or mutant ALK enzyme, and 7.8−2,000 μM YFF peptide and 1 mM ATP to generate $K_{M,YFF}$ or 7.8−1,600 μM ATP and 1 mM YFF peptide to generate $K_{M,ATP}$. Reactions were started by adding ATP and conducted at 30 °C. Initial reaction velocities were fit to a Michalis-Menten equation using GraphPad Prism (GraphPad Software, San Diego, CA) to determine the turnover number, $k_{cat}$, and Michaelis constants, $K_M$, for ATP and YFF substrate.

**Crystallography.** Non-phosphorylated human wildtype and mutant ALK kinase domains proteins (amino acids 1093−1411) were crystallized by the hanging drop vapor diffusion method at 13 °C by mixing equal volumes of protein solution (11−15 mg/mL) with a crystallization solution containing 0.15 M ammonium sulfate, 9−10.5% (w/v) monomethyl ether polyethylene glycol) (MW 5000) and 0.1 M 2-(*N*-morpholino)-ethanesulfonic acid (MES) buffer in a pH range of 5.3−5.6 for wildtype and 0.2 M lithium sulfate, 20−21% (w/v) poly(ethylene glycol) (MW 3350), 0.1% (w/v) β-octylglucoside and 0.1 M Tris at pH 8.4−8.5 for L1196M and C1156Y ALK. Crystals were flash frozen in liquid nitrogen and x-ray diffraction was collected at Argonne National Laboratories Advanced Photon Source Beamline 17-ID. The structures were initially solved using the previously described ALK-crizotinib structure (PDB ID = 2XP2)[4] as the starting model for refinement with CNX 2005.[5] Rigid body refinement, simulated annealing, and multiple rounds of model building followed by positional and isotropic restrained B-factor refinement was conducted. Structural statistics are included in Table S1. The structures have

been deposited to the PDB with accession codes: 6CDT (wildtype), 2YJS (C1156Y) and 2YHV (L1196M).

**Table S1. Crystallography methods and statistics.**

| ALK KD structure | wildtype | L1196M | C1156Y |
|---|---|---|---|
| PDB ID | 6CDT | 2YHV | 2YJS |
| space group | P 21 21 21 | P 21 21 21 | P 21 21 21 |
| **Unit cell** | | | |
| a (Å) | 52.02 | 52.1 | 51.95 |
| b (Å) | 57.47 | 57.76 | 57.16 |
| c (Å) | 104.73 | 105.19 | 104.9 |
| | | | |
| **Diffraction data**[a] | | | |
| resolution range (Å) | 105−1.79 | 105−1.89 | 105−1.84 |
| observations | 184266 | 166821 | 179128 |
| unique reflections | 29890 | 25946 | 28015 |
| completeness (%) | 99.9 (99.0) | 99.8 (99.9) | 100 (100) |
| $\langle I/\sigma_i \rangle$ | 32.8 (3.8) | 18.7 (3.9) | 23.3 (4.0) |
| $R$ (%)[b] | 5.5 (29.1) | 6.2 (47) | 4.8 (50.0) |
| | | | |
| **Refinement statistics** | | | |
| resolution range (Å) | 36−1.80 | 52−1.90 | 52−1.90 |
| reflections used | 29196 | 25657 | 25321 |
| $R$ factor , $R_{free}$ (%)[c] | 19.6, 22.6 | 20.7, 23.8 | 21.2, 24.3 |
| rmsd bond lengths (Å) | 0.004 | 0.004 | 0.004 |
| rmsd bond angles (°) | 0.8 | 0.8 | 0.8 |
| mean isotropic B (Å$^2$) | 28.7 | 31.2 | 30.4 |

[a] Values in parentheses refer to the highest resolution shell.

[b] $R = \Sigma |\langle I \rangle - I| / \Sigma I$ where $I$ is measured intensity for reflections with indices hkl.

[c] R factor = $100 \times \Sigma |F_o - F_c| / \Sigma |F_o|$; $R_{free}$ = free R-factor based on random 3−5% of all data.

**Normalized B-factors.** Normalized B-factors were computed with a Python 3.5 script utilizing the commercial OEChem toolkit (https://docs.eyesopen.com/toolkits/python/oechemtk/index.html) for cheminformatics operations (loading molecular structures, identifying relevant atoms/residues, and extracting B-factors), and the open source numpy package (http://www.numpy.org) for calculating the average and standard deviation.

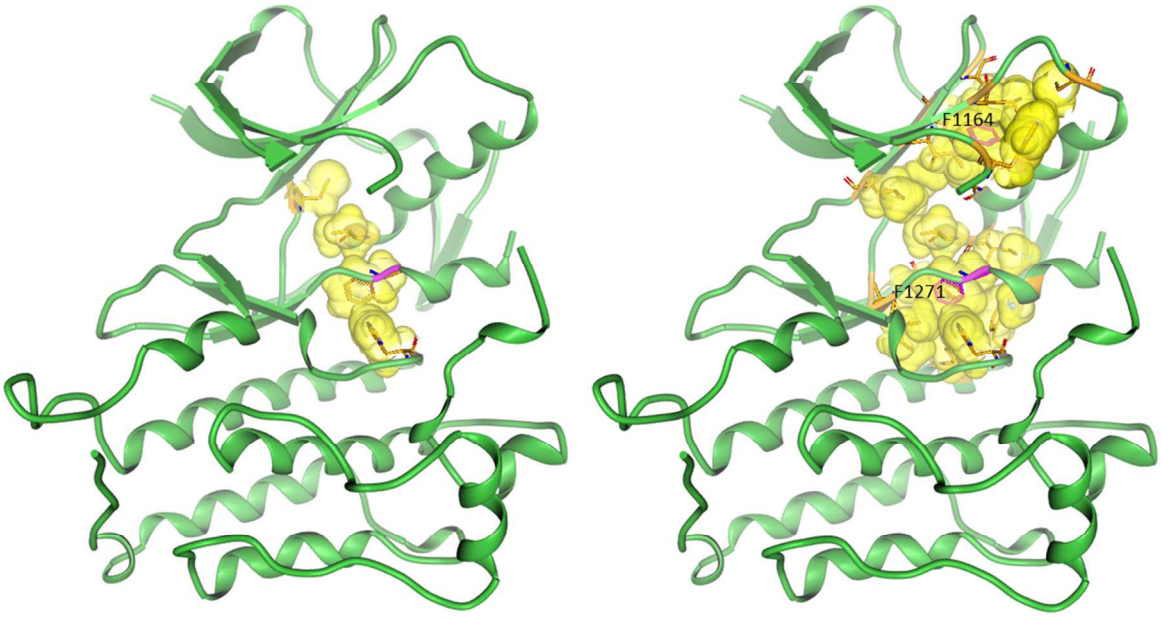


Figure S1. ALK apo crystal structure (PDB code 6CDT). Left panel: Regulatory-spine (R-spine) residues with van der Waals surface in yellow. Right panel: R-spine and hydrophic clusters centered on F1164 and F1271.

**Molecular Dynamics Simulations**. The MD simulations were performed using Desmond (Schrodinger) program. MD simulations for each protein were performed with the following schedule: a 50 ns equilibrium run followed by a 50 ns production run. The OPLS3 Force Field was used. In addition, the TIP3P model was used for solvating the entire complex at pH 7. Moreover, NVT ensemble (P = 1 atm, T = 300 K) was chosen for all simulations. Samplings of results were done at every 200 step during the simulation. A 15 Å cutoff was used for the long-range electrostatic interactions. The time step was set to 2.0 fs. During the equilibration, the system was gradually heated with the main chains constrained by 5 kcal/mol Å in the NVT ensemble from 0 to 300 K (using Nose-Hoover Thermostat). The atom coordinates were collected at the interval of 5 ps for the last 50 ns to analyze the structures in detail. The MD trajectories of the WT and other mutant systems were generated. The atomic RMSDs of the protein structures were calculated from the first frame of the production run (equilibrated structures) as a function of time. RMSF values were also calculated.

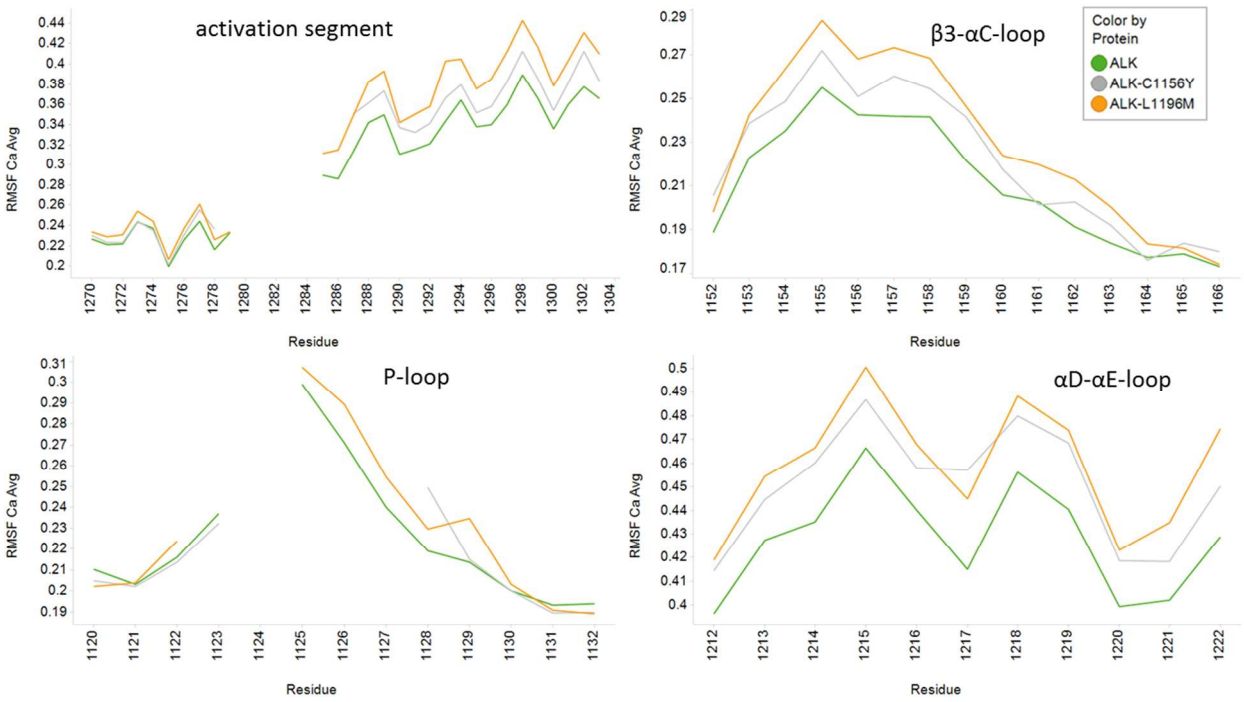


Figure S2. MD simulation of ALK (green), ALK-C1156Y (gray), and ALK-L1196M (orange). Triplicate average of Cα atom RMSF values show greater motion in mutants over wildtype in key regions of the protein.

**Hydrogen Deuterium Exchange Mass Spectrometry (HDX-MS).** Three ALK constructs (WT, C1156Y, L1196M, 1093−1411) were provided in stock buffer (25 mM Hepes, pH 7.2, 150 mM NaCl, 2 mM TCEP, 5% glycerol) and subsequently diluted to 0.5 mg/ml in working buffer (10 mM Tris, 50 mM NaCl, pH 7.2) for HDX-MS analysis. Deuterium exchange was conducted on a temperature-controlled HDX2 auto-sampler (Leap Technologies). Aliquots of sample (4 µL) were mixed (1:5) with deuterium exchange buffer ($D_2O$ 10 mM Tris, 50 mM NaCl, pH 7.2) at 4 °C. Exchange was conducted across five time points (10 s, 60 s, 360 s, 3600 s, 43200 s) and run in triplicate. After each defined exchange time, the sample is transferred by a chilled syringe, and quenched/denatured at 1 °C with addition of 20 µL of chilled quench buffer (3.2 M guanidine hydrochloride, 0.8% formic acid). Quenched samples were injected into the chiller box, which housed the sample loop, protease column and trap/analytical columns at 3 °C. Blank injections were inserted between every sample to minimize potential carryover.

A three pump scheme was employed for peptide detection using Vanquish UPLC pumps (Dionex). A loading pump running 0.1% formic acid at 200 µL/min carried sample sequentially across the pepsin/protease XIII immobilized column (NovaBio Assay) and 2.1 x 5 mm CSH C18 trap column(Waters) for 2 minutes. Peptides were desalted for an additional 30 seconds, while the protease column was back-flushed with 0.05% TFA. Peptides were subsequently eluted/separated across a Kinetex C18 2.1 x 30 mm 1.3 micron analytical column via a 5.7

minute gradient of mobile phase B (8%−37% ACN, 0.1% formic) employing a binary pump gradient with mobile phase A (0.1% formic acid) and mobile phase B (acetonitrile 0.1% formic acid) at 150 µL/min.

Data acquisition and processing involved multiple software platforms. Mass spectra were acquired on a Thermo Fusion-Lumos mass spectrometer running XCalibur 2.1 across a scan range of 375−1300 m/z. Orbitrap resolution was set at 60,000 for charge state selection of +2 − +5 peptides. Peptide fragmentation for peptide identification employed HCD tandem MS2 acquisition. Electrospray source settings were set at high gas flow (27 sheath, 9 aux) and lowered temperature (150 °C) to handle the 150 µL/min LC flow rate, while minimizing potential deuterium back-exchange. Peptide pools were generated in Thermo Proteome Discoverer 2.1 with a directed search against the ALK WT (1093−1411) sequence, using a Sequest HT search and a fixed value PSM validator (0.05 Delta Cn). Tolerances were set at 5 ppm mass accuracy with 0.6 Da fragments, which provided ALK WT sequence coverage of 95.72%. Deuterium exchange for each time point was determined for this peptide pool using HDExaminer 2.2 software. For peptide deuterium uptake, the first two residues and prolines were excluded from calculations.

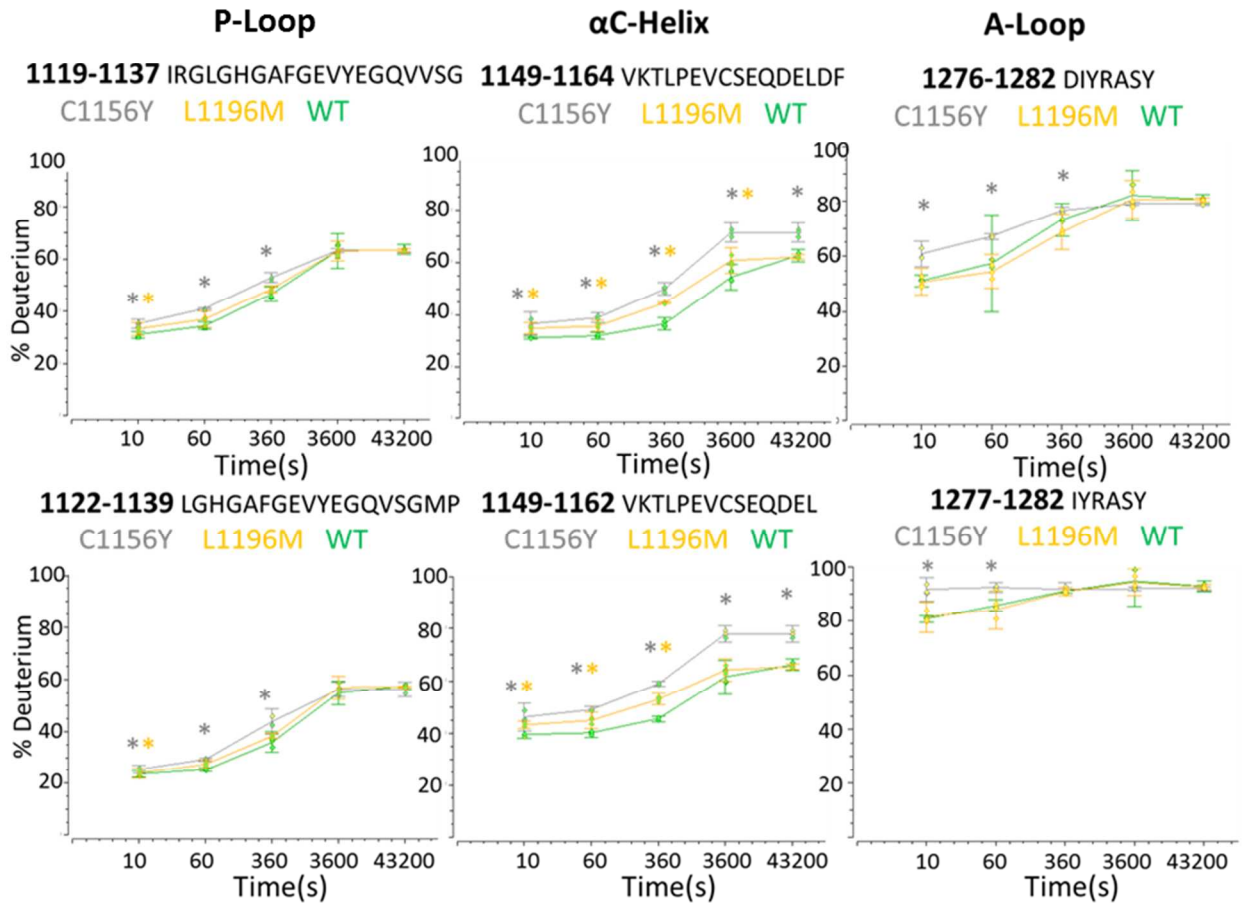

Figure S3. Overlaid deuterium peptide plots for ALK-WT (green), C1156Y (gray) and L1196M (orange) illustrate comparative percentage deuterium uptake across five exchange time points (10 s, 60 s, 360 s, 1 h, 12 h). Representative peptides for selected regions (P-loop, αC-helix, and activation loop) reflect enhanced uptake for C1156Y and L1196M. Asterisks represent significant differences.

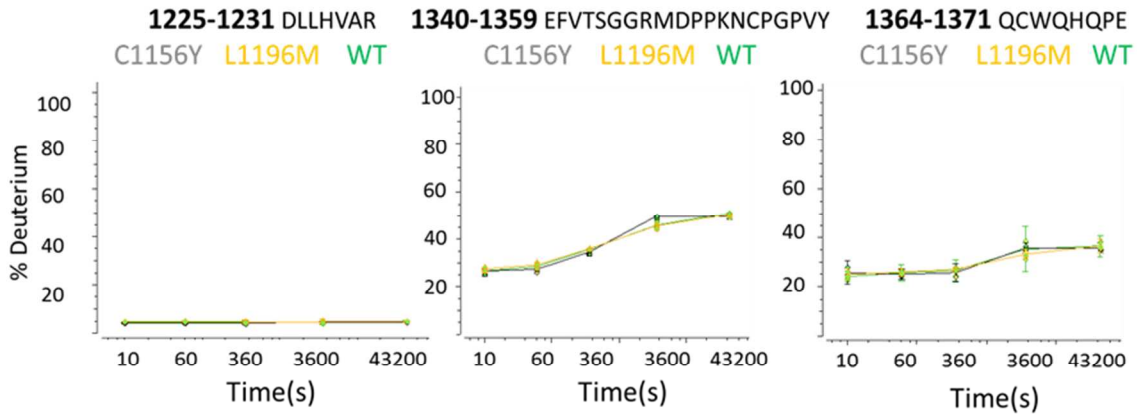


Figure S4. Overlaid deuterium peptide plots for ALK-WT (green), C1156Y (gray) and L1196M (orange) illustrate comparative percentage deuterium uptake across five exchange time points (10 s, 60 s, 360 s, 1 h, 12 h). Representative peptides for selected regions that reflect no significant difference in uptake for C1156Y and L1196M, shown as negative control.

1. Shaw, A. T.; Friboulet, L.; Leshchiner, I.; Gainor, J. F.; Bergqvist, S.; Brooun, A.; Burke, B. J.; Deng, Y. L.; Liu, W.; Dardaei, L.; Frias, R. L.; Schultz, K. R.; Logan, J.; James, L. P.; Smeal, T.; Timofeevski, S.; Katayama, R.; Iafrate, A. J.; Le, L.; McTigue, M.; Getz, G.; Johnson, T. W.; Engelman, J. A., Resensitization to Crizotinib by the Lorlatinib ALK Resistance Mutation L1198F. *N Engl J Med* **2016,** *374* (1), 54-61.
2. Timofeevski, S. L.; McTigue, M. A.; Ryan, K.; Cui, J.; Zou, H. Y.; Zhu, J. X.; Chau, F.; Alton, G.; Karlicek, S.; Christensen, J. G.; Murray, B. W., Enzymatic characterization of c-Met receptor tyrosine kinase oncogenic mutants and kinetic studies with aminopyridine and triazolopyrazine inhibitors. *Biochemistry* **2009,** *48* (23), 5339-49.
3. Donella-Deana, A.; Marin, O.; Cesaro, L.; Gunby, R. H.; Ferrarese, A.; Coluccia, A. M.; Tartari, C. J.; Mologni, L.; Scapozza, L.; Gambacorti-Passerini, C.; Pinna, L. A., Unique substrate specificity of anaplastic lymphoma kinase (ALK): development of phosphoacceptor peptides for the assay of ALK activity. *Biochemistry* **2005,** *44* (23), 8533-42.
4. Huang, Q.; Johnson, T. W.; Bailey, S.; Brooun, A.; Bunker, K. D.; Burke, B. J.; Collins, M. R.; Cook, A. S.; Cui, J. J.; Dack, K. N.; Deal, J. G.; Deng, Y. L.; Dinh, D.; Engstrom, L. D.; He, M.; Hoffman, J.; Hoffman, R. L.; Johnson, P. S.; Kania, R. S.; Lam, H.; Lam, J. L.; Le, P. T.; Li, Q.; Lingardo, L.; Liu, W.; Lu, M. W.; McTigue, M.; Palmer, C. L.; Richardson, P. F.; Sach, N. W.; Shen, H.; Smeal, T.; Smith, G. L.; Stewart, A. E.; Timofeevski, S.; Tsaparikos, K.; Wang, H.; Zhu, H.; Zhu, J.; Zou, H. Y.; Edwards, M. P., Design of potent and selective inhibitors to overcome clinical anaplastic lymphoma kinase mutations resistant to crizotinib. *J Med Chem* **2014,** *57* (4), 1170-87.
5. Brunger, A. T.; Adams, P. D.; Clore, G. M.; DeLano, W. L.; Gros, P.; Grosse-Kunstleve, R. W.; Jiang, J. S.; Kuszewski, J.; Nilges, M.; Pannu, N. S.; Read, R. J.; Rice, L. M.; Simonson, T.; Warren, G. L., Crystallography & NMR system: A new software suite for macromolecular structure determination. *Acta Crystallogr D Biol Crystallogr* **1998,** *54* (Pt 5), 905-21.